

A Mode-Based Averaged Power Converter Model for Large Transients^{*}

Adam Kastner^{*} Lutz Gröll^{*} Veit Hagenmeyer^{*}

^{*} Karlsruhe Institute of Technology, Karlsruhe, Germany (e-mail: {adam.kastner, lutz.groell, veit.hagenmeyer}@kit.edu)

Abstract: Power converters employ high-frequency switching between multiple switch states, each of which causes the system to exhibit a different dynamic behavior. Averaged models are a common simplification used for describing the behavior in one or two specific cycles of switch states, also called operating modes. In this context, we propose extending the method of Sun et al. (2001), which allows averaging in two operating modes, to a converter model with four operating modes. We show in simulations that our model results in a reasonable approximation of the true moving average of the original switching converter model during large transients that pass through multiple operating modes.

Copyright © 2022 The Authors. This is an open access article under the CC BY-NC-ND license (<https://creativecommons.org/licenses/by-nc-nd/4.0/>)

Keywords: power converters, switched systems, averaging, simulation

1. INTRODUCTION

Most switching power converter types contain both controlled switches, such as transistors, and uncontrolled switches, such as diodes. Under the periodic operation of the controlled switches using pulse-width modulation (PWM), the system cycles through a series of switch states. Different cycles of switch states may occur in the same converter topology depending on its state and input and are referred to as operating modes of the converter (Maksimovi and uk, 1991).

Besides the so-called continuous conduction mode (CCM), where only controlled switchings occur, there exist also so-called discontinuous modes, in which a diode causes additional switchings. In a converter with one transistor and one diode, discontinuous inductor current mode (DICM), also called discontinuous conduction mode (DCM), discontinuous capacitor voltage mode (DCVM), and discontinuous quasi-resonant mode (DQRM) are possible (Maksimovi and uk, 1991). DQRM is also called double discontinuous mode (DDM) (Sadarnac et al., 2004) and for buck converters with LC input filter, DCVM is also called discontinuous input voltage mode (Lee et al., 1997).

While the modes are commonly called discontinuous modes, it is important to note that the system states, which correspond to inductor currents and capacitor voltages, are still continuous functions of time, but clamped to zero during certain intervals.

Discontinuous modes may occur during transients even between CCM operating points, as was already discussed by Erickson et al. (1982). While stationary discontinuous modes are a result of the finite frequency of the controlled switching and can be eliminated by reducing the PWM period, transient DICM and DCVM modes can still occur when the PWM period tends to zero.

In this context, the transition between averaged models of CCM and DICM was considered in Sun (2000). Their work was also extended to models including parasitic effects by Davoudi and Jatskevich (2007) and an adjusted discrete-time mode transition law was suggested by Li et al. (2016). To the best knowledge of the authors however, no averaged model that also covers the transitions to DCVM and DDM exists so far in the literature.

Note, that not all four discrete states occur in all converter types, and therefore some types of discontinuous modes will only occur in specific topologies. In the two-state buck converter, the transistor and diode never conduct current at the same time. Converters where all four discrete states can occur include the Ćuk converter (4 states) and the buck converter with LC input filter (4 states), the latter is the focus of the present paper.

The paper is organized as follows: In Sec. 2, a switching model for the four discrete states is developed. Section 3 extends the averaging method of Sun et al. (2001) to the DCVM and DDM, and we show in Sec. 4 the three other modes can be considered as special cases of the developed DDM model. The results of two simulations are used to compare the mode-based averaged model with the non-averaged switching model in Sec. 5.

2. NON-AVERAGED SWITCHING MODEL

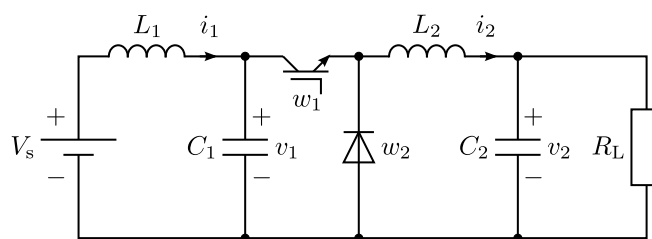


Fig. 1. Electrical circuit of the Buck converter with LC input filter

^{*} This work was supported by the Helmholtz Association under the Innovation Pool Project “Energy Transition and Circular Economy”.

The mathematical model of the buck converter with LC input filter is based on the circuit diagram in Fig. 1. We assume linear time-invariant behavior for the passive elements and that both switching elements, the transistor and the diode, act as ideal switches, i.e. have no resistance when conducting and infinite resistance when blocking. The transistor's behavior is controlled via the input $w_1 \in \{0,1\}$, while the switch state $w_2 \in \{0,1\}$ of the diode changes autonomously whenever the forward current or the reverse voltage reach zero.

Dynamic equations which use the currents in inductors and voltages over capacitors as states can be obtained using Kirchoff's laws. We apply a normalization as described by Sira-Ramírez and Silva-Ortigoza (2006) to reduce the number of model parameters and work with dimensionless variables in the control notation. With the factors

$$\kappa := V_s \sqrt{\frac{C_1}{L_1}}, \quad \theta := \sqrt{L_1 C_1}, \quad (1)$$

we define the normalized states and time as

$$x_1 := \frac{i_1}{\kappa}, \quad x_2 := \frac{v_1}{V_s}, \quad x_3 := \frac{i_2}{\kappa}, \quad x_4 := \frac{v_2}{V_s}, \quad \tau := \frac{t}{\theta}. \quad (2)$$

Moreover, the dot notation $\dot{x} := \frac{dx}{d\tau}$ refers to the state derivative with respect to the normalized time variable.

The normalization enables expressing the dynamics considering only three dimensionless parameters

$$p_1 := \frac{L_1}{L_2}, \quad p_2 := \frac{C_1}{C_2}, \quad p_3 := \frac{1}{R_L} \sqrt{\frac{L_1}{C_1}}. \quad (3)$$

The PWM period T_{PWM} is also normalized, resulting in a fourth parameter $T = \frac{T_{\text{PWM}}}{\theta}$. For interpretation of the results from analysis or simulation, the normalized system variables can be transformed back into physical quantities:

$$i_1 = \kappa x_1, \quad v_1 = V_s x_2, \quad i_2 = \kappa x_3, \quad v_2 = V_s x_4, \quad t = \theta \tau. \quad (4)$$

Due to the two switching elements, four different continuous dynamics can occur. In hybrid modeling, each of these dynamics is associated with one discrete state or location, and we say that the system is in discrete state j , $j = 1, 2, 3, 4$ while the j th continuous dynamic determines the state trajectories (Heemels et al., 2009). In other applications, these discrete states might be referred to as operating modes, the power electronics literature however uses the term mode to refer to the four sequences of discrete states that can occur within one PWM cycle.

Figure 2 shows the four discrete states and the state and input conditions under which the system switches to a different discrete state, as well as the four cycles which constitute the operating modes. We use the same indexing as Sun et al. (2001) for the first three discrete states, as shown in Tab. 1, and label the state where both transistor w_1 and diode w_2 are conducting with $j = 4$.

The dynamics in each discrete state take the form of an affine differential equation

$$\dot{x} = A_j x + b, \quad (5)$$

in which the system matrices take the form

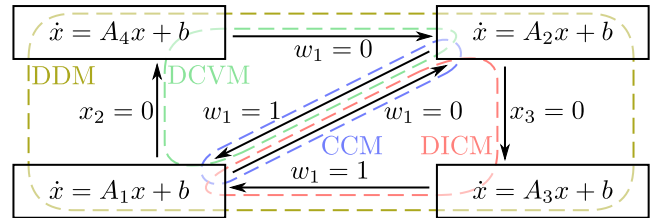


Fig. 2. Discrete states, switch conditions and cycles of the operating modes

$$A_1 = \begin{bmatrix} 0 & -1 & 0 & 0 \\ 1 & 0 & -1 & 0 \\ 0 & p_1 & 0 & -p_1 \\ 0 & 0 & p_2 & -p_2 p_3 \end{bmatrix}, \quad A_2 = \begin{bmatrix} 0 & -1 & 0 & 0 \\ 1 & 0 & 0 & 0 \\ 0 & 0 & 0 & -p_1 \\ 0 & 0 & p_2 & -p_2 p_3 \end{bmatrix}, \quad (6a)$$

$$A_3 = \begin{bmatrix} 0 & -1 & 0 & 0 \\ 1 & 0 & 0 & 0 \\ 0 & 0 & 0 & 0 \\ 0 & 0 & 0 & -p_2 p_3 \end{bmatrix}, \quad A_4 = \begin{bmatrix} 0 & 0 & 0 & 0 \\ 0 & 0 & 0 & 0 \\ 0 & 0 & 0 & -p_1 \\ 0 & 0 & p_2 & -p_2 p_3 \end{bmatrix}, \quad (6b)$$

$$b = \begin{bmatrix} 1 \\ 0 \\ 0 \\ 0 \end{bmatrix}. \quad (6c)$$

The method in Sun et al. (2001) assumes implicitly that an all-zero column is placed in the system matrix where the constant-zero state is located, which is the third column of A_3 and the second column of A_4 .

3. AVERAGED OPERATION MODE MODELS

Switching introduces high-frequency components, commonly referred to as “ripple”, into the states of the model. To isolate the low-frequency components of interest and discard the undesirable ripple, a moving average of the states

$$x_{\text{MA}} = \frac{1}{T} \int_{\tau-T/2}^{\tau+T/2} x(\sigma) d\sigma, \quad (7)$$

also called sliding average in Bacha et al. (2014), can be used.

The purpose of averaging methods is to provide a dynamic model for an averaged state \bar{x} which approximates the true moving average of the non-averaged switching model. The input $u \in [0, 1]$ of this averaged model approximates the moving average $w_{1,\text{MA}}$ of the switch-controlling input. While the actual moving average can only change in restricted ways due to the discrete-time nature of PWM, we assume the new input u to be a continuous variable, such that the averaged model takes the form of a nonlinear differential equation

$$\dot{\bar{x}} = f(\bar{x}, u). \quad (8)$$

Table 1. Mapping from discrete state index to switch configuration

| discrete state | w_1 | w_2 |
|----------------|-------|-------|
| 1 | 1 | 0 |
| 2 | 0 | 1 |
| 3 | 0 | 0 |
| 4 | 1 | 1 |

A commonly used technique is state space averaging (Middlebrook and uk, 1977), which uses a weighted average of the dynamics associated with the discrete states as dynamics for the averaged states. For a converter with only controlled switching between two discrete states with linear dynamics, the state space averaged model reads as

$$\dot{\bar{x}} = (uA_1 + (1-u)A_2)x + b. \quad (9)$$

The basic state space averaging method makes use of the small-ripple approximation, which is not valid for discontinuous modes. Sun et al. (2001) introduced a “modification matrix” M in state space averaging for DICM based on the observations about circuit averaging in Sun (2000), and we extend this method to the cases of DCVM and DDM: With a modification matrix, the dynamics for the averaged system become

$$\dot{\bar{x}} = (d_1A_1 + d_2A_2 + d_3A_3 + d_4A_4)Mx + b, \quad (10)$$

where d_j is the relative active duration in the averaging period of the discrete state j . Considering that $d_1 + d_4 = u$ and $d_2 + d_3 = 1 - u$, we can interpret (10) as a model with an external input u , and two virtual inputs d_1 and d_2 , i.e.

$$\begin{aligned} \dot{\bar{x}} &= \tilde{f}(\bar{x}, u, d_1, d_2) \\ &= (d_1A_1 + d_2A_2 \\ &\quad + (1-u-d_2)A_3 + (u-d_1)A_4)M\bar{x} + b. \end{aligned} \quad (11)$$

Since a current or voltage does not affect the other states in the time interval during which it is zero, Sun et al. (2001) proposes considering only the intervals during which the respective state is nonzero when calculating its influence on other states. Thus, the matrix M increases the effective magnitude $\bar{x}_{\text{eff}} = M\bar{x}$ of the states which have a constant-zero interval accordingly.

In this context, Sun (2000) proposed a method to calculate $d_2(\bar{x}, u)$ in both CCM and DICM as a nonlinear state feedback. We extend this method to calculate the duty ratios in DCVM based on the duality principle (Ćuk, 1979), and further to DDM by introducing a more general signal model. The effective duty ratios $d_1(\bar{x}, u)$ and $d_2(\bar{x}, u, d_1)$ obtained for DDM are shown to be valid for all four operation modes when considering physical limitations in Sec. 4.

Note that other averaging methods for converters including discontinuous modes exist and may offer better accuracy than Sun et al.’s improved averaging method (Mao et al., 2018). They are, however, not considered in the present paper, as the extension of the method in Sun et al. (2001) guarantees a continuous transition between the assumed signal shapes and therefore a continuous vector field at the mode boundaries.

In both DCVM and DDM, the same piecewise linear shape for x_2 is assumed, as shown in Fig. 3. For averaging purposes, we assume that the states x_1 and x_4 can be approximated by their respective moving averages \bar{x}_1 and \bar{x}_4 . In DCVM, this assumption will also hold for $x_3 \approx \bar{x}_3$. In DDM, we assume a piecewise linear signal shape for both x_2 and x_3 .

Note that the assumption of piecewise linear signal shapes can be accurate for DICM and DCVM modes when only one state variable has large ripple. When ripple is large in both x_2 and x_3 , such as in the DDM, the actual signal

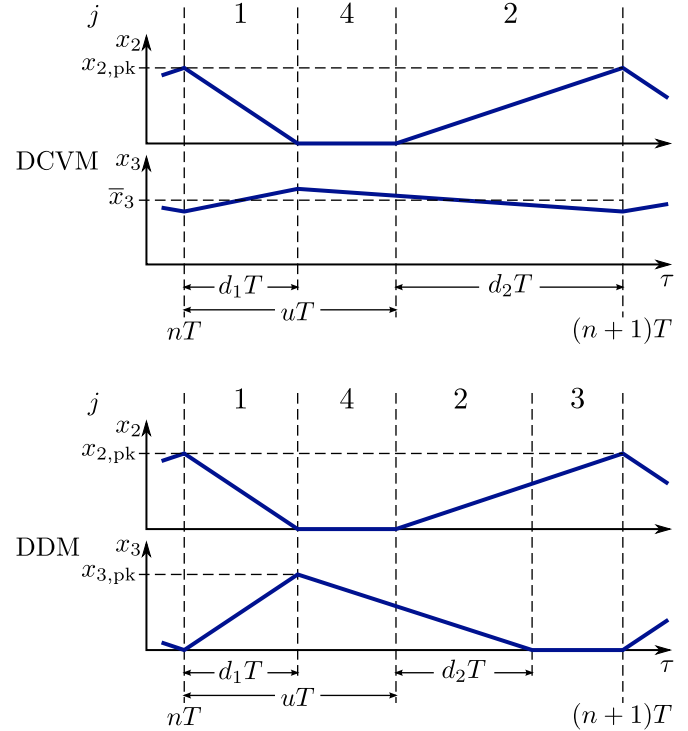


Fig. 3. Assumed signal shapes in DCVM and DDM

shapes of during the first interval d_1T are sinusoidal arcs (Maksimovi and uk, 1991). While assuming only piecewise linear signal shapes in all modes introduces an inaccuracy into the calculation of the effective duty ratios, it allows the mode-specific models to coincide in the boundary cases when $d_1 = u$ or $d_2 = 1 - u$.

As the proportion of time during which the respective state is nonzero is $1 - u + d_1$ for x_2 and $u + d_2$ for x_3 , the modification matrix for our system is

$$M = \text{diag} \left(1, \frac{1}{1-u+d_1}, \frac{1}{u+d_2}, 1 \right). \quad (12)$$

In both DCVM and DDM, we calculate the peak value

$$x_{2,\text{pk}} = \bar{x}_1(1-u)T, \quad (13)$$

achieved in one switching cycle based on the slope and duration of the rising segment in discrete states 2 and 3. Using the signal shape assumption, the average is

$$\bar{x}_2 = \frac{(d_1 + (1-u))x_{2,\text{pk}}}{2}, \quad (14)$$

which can be used to obtain the effective duty ratio of discrete state 1

$$d_1 = \text{sat}_0^u \left(\frac{2\bar{x}_2}{\bar{x}_1(1-u)T} - (1-u) \right). \quad (15)$$

As the duty ratio of the first switch state is restricted to the interval $[0, u]$, we apply a saturation function

$$\text{sat}_a^b(x) = \begin{cases} b, & b < x \\ x, & a \leq x \leq b. \\ a, & x < a \end{cases} \quad (16)$$

In DCVM, $d_2 = 1 - u$, and for DDM we calculate d_2 from the signal shape given in Fig. 3. For the peak value

$$x_{3,\text{pk}} = p_1 \left(\bar{x}_4 - \frac{\bar{x}_2}{1-u+d_1} \right) d_1T, \quad (17)$$

we consider the rising slope in discrete state 1, but we use the adjusted average $x_{2,\text{eff}} = \frac{\bar{x}_2}{1-u+d_1}$. From the relation between average and peak values

$$\bar{x}_3 = \frac{(u+d_2)x_{3,\text{pk}}}{2}, \quad (18)$$

the effective duty ratio of discrete state 2

$$d_2 = \text{sat}_0^{1-u} \left(\frac{2\bar{x}_3}{p_1(\bar{x}_4 - \bar{x}_2/(1-u+d_1))d_1T} - u \right) \quad (19)$$

is calculated.

The calculated effective duty ratios form a state feedback for the system (11) with three inputs u , d_1 and d_2 . This leads to an averaged model in the desired form of $\dot{\bar{x}} = f(\bar{x}, u)$.

4. MODE-BASED AVERAGED MODEL

The averaged models for all other operating modes can be interpreted as special cases of the DDM model. If the argument to the saturation function in (19) is $\tilde{d}_2 > 1-u$, we have $d_2 = 1-u$ and obtain the DCVM model. In the case where $\tilde{d}_1 > u$ before saturation, we obtain $d_1 = u$ and

$$d_2 = \text{sat}_0^{1-u} \left(\frac{2\bar{x}_3}{p_1(\bar{x}_4 - \bar{x}_2)d_1T} \right)$$

because $\bar{x}_{2,\text{eff}} = \bar{x}_2$, which is identical to the model for DICM in Sun et al. (2001).

When both $\tilde{d}_1 > u$ and $\tilde{d}_2 > 1-u$, (11) simplifies to the CCM state-space averaged model (9). A similar relation was already shown in Sun (2000) between the DICM and CCM models. This allows for using the DDM model with duty ratio saturations as a merged averaged model for all modes.

The merged averaged model represents four nonlinear models for the four operating modes with discrete switching between them. This is illustrated in Fig. 4, where \tilde{d}_1 and \tilde{d}_2 refer to the values calculated in (15) and (19) before applying the saturation function (16).

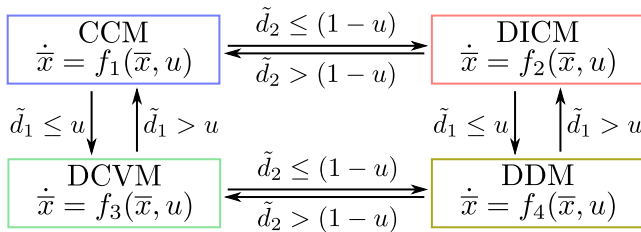


Fig. 4. Operating modes and transitions in the mode-based averaged model

The four vector fields

$$f_1(\bar{x}, u) = \tilde{f}(\bar{x}, u, u, 1-u) \quad (20a)$$

$$f_2(\bar{x}, u) = \tilde{f}(\bar{x}, u, u, \tilde{d}_2) \quad (20b)$$

$$f_3(\bar{x}, u) = \tilde{f}(\bar{x}, u, \tilde{d}_1, 1-u) \quad (20c)$$

$$f_4(\bar{x}, u) = \tilde{f}(\bar{x}, u, \tilde{d}_1, \tilde{d}_2) \quad (20d)$$

are obtained by inserting the appropriate values for d_1 and d_2 for the virtual inputs of (11) depending on whether they are saturated or not. For the sake of readability, we have

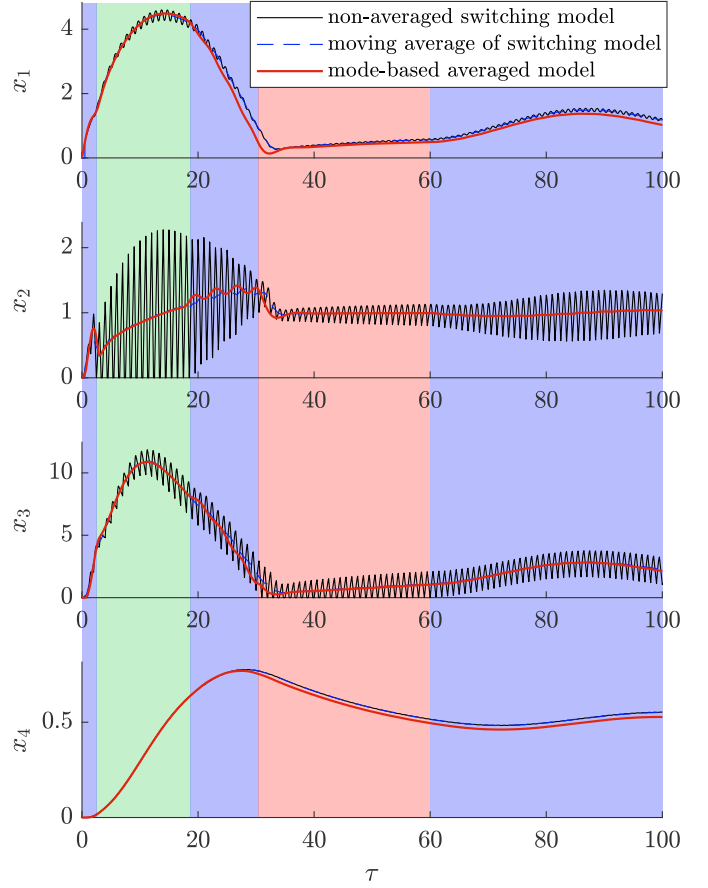


Fig. 5. Simulated state trajectories for parameters (21), with time intervals colored according to operating mode: CCM in blue, DCVM in green, DICM in red

not included the lower saturation of zero in (20), although it should likewise be included in f_2 , f_3 and f_4 .

An important feature of our model is the continuity of the vector field at the mode boundaries, e.g.

$$f_1(\bar{x}, u)|_{\tilde{d}_1=u} = f_3(\bar{x}, u)|_{\tilde{d}_1=u},$$

which is guaranteed due to the continuity of the saturation function (16). This ensures that no sliding modes can occur in the mode-based averaged model.

5. SIMULATION RESULTS

The models presented in Sec. 2 and Sec. 4 are implemented using the software package MATLAB/Simulink. The non-averaged switching model uses a Stateflow chart with continuous-time embedded dynamics and the merged averaged model is implemented using a MATLAB function implementing (15), (19), and (11).

5.1 State trajectory approximation during large transients

To simulate multiple mode transitions during a transient, the parameters

$$p_1 = 8, \quad p_2 = 0.005, \quad p_3 = 4, \quad T = 1 \quad (21)$$

are used. For an input step from 0 to 0.5 at normalized time $\tau = 0$ with initial states $x(0) = \bar{x}(0) = 0$, the state trajectories of the switching model, its moving average, and of the merged averaged model are shown in Fig. 5.

Starting from a zero initial state, the system enters the DCVM after a very short time in CCM. At approximately $\tau = 18$, the system returns to CCM operation only to enter into DICM between approximately $\tau = 30$ and $\tau = 60$, before finally returning to CCM. The new merged averaged model follows the moving average of the switching model closely. The offset between averaged and switching model observed in the first and fourth state variable is a consequence of the approximations made in the averaging process.

State trajectories of a simulation with parameters

$$p_1 = 80, \quad p_2 = 0.005, \quad p_3 = 20, \quad T = 1 \quad (22)$$

for an input step from 0 to 0.5 at $\tau = 0$ are shown in Fig. 6, demonstrating the transition to DDM. The system

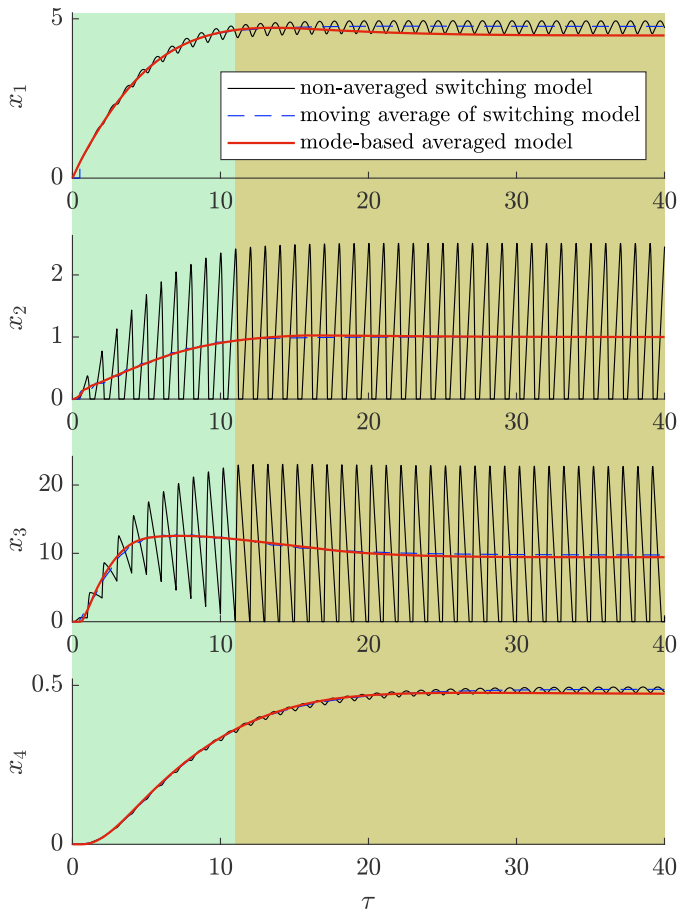


Fig. 6. Simulated state trajectories for parameters (22), with time intervals colored according to operating mode: DCVM in green, DDM in yellow

first enters the DCVM and then operates in the DDM from $\tau = 11$ onwards. In this case, the state trajectories of the developed mode-based averaged model also stay close to the moving average of the states of the switched model.

5.2 Quality of the the effective duty ratio's approximation

The averaged models introduced in Sec. 3 calculate effective duty ratios d_1 and d_2 based on a piecewise linear signal model. Originally, it was proposed in Sun et al. (2001) for DICM based on the assumption that only the inductor current shows large ripple.

When a system has large ripple in both voltage and current, which can occur in all operating modes and is always the case in DDM, this introduces errors in the calculation of the effective duty ratios.

Figure 7 compares the effective duty ratios calculated in the averaged model with those resulting from the transitions of the switching model for the simulation with parameters (21). While the averaged model shows the same quality of change in the duty ratios at approximately the same time, a slight difference in magnitudes can be observed during the intervals of DCVM and DICM operation.

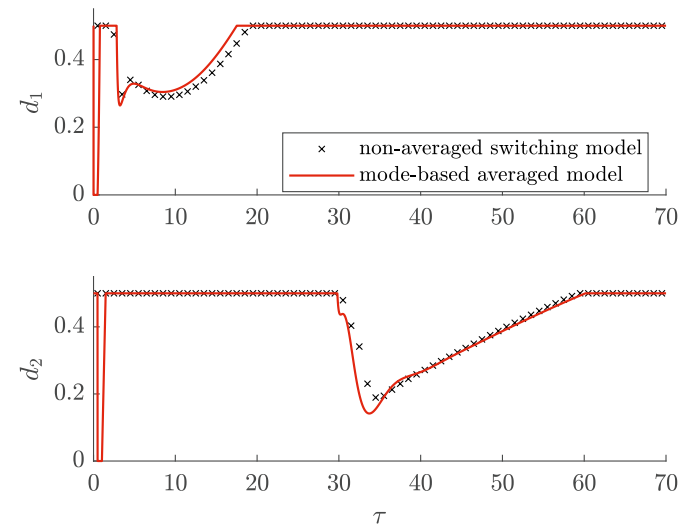


Fig. 7. Simulated duty ratios with parameters (21)

While the states of the averaged model are still close to the moving averages of the switching model with the parameters of (22), the quantitative difference in the effective duty ratios becomes more obvious in Fig. 8, as not only the magnitude of the effective duty ratio is different, but also the time at which d_2 decreases below 0.5 and the system enters into DDM.

As many power converters are designed to operate mainly in CCM and DCM, the large deviations for DDM visible in the second simulation would not be a major concern when the system only enters this mode for short periods during transients. Our simulation shows a close approximation of the signals under the occurrence of both DCVM and DICM when entering a CCM operating point. The steady-state difference introduced by inaccuracies in averaging would be compensated in a closed-loop system by a controller incorporating integral action.

6. CONCLUSION AND OUTLOOK

The present paper shows the applicability of designing an averaged model for large transients of power converters which include multiple operating modes. The developed model matches closely the moving average of the states of the switching model and the reduced effective duty ratios in areas where the modeling assumptions are accurate. Such a mode-based averaged model is well-suited for simulation in cases where large transients have to be

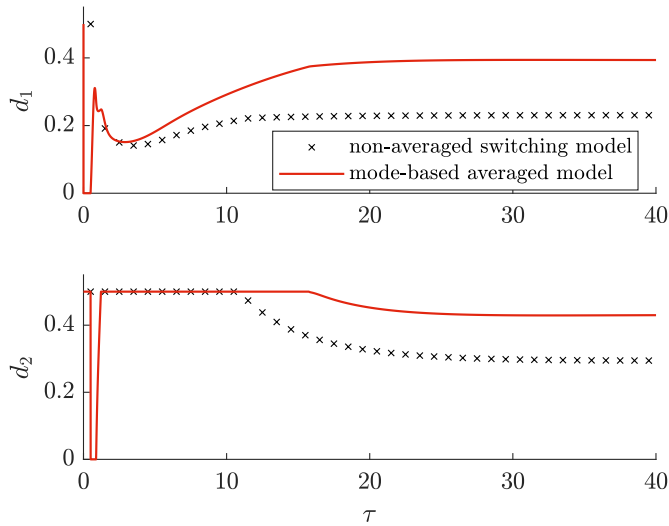


Fig. 8. Simulated duty ratios with parameters (22)

considered but the non-averaged switching model is too computationally expensive.

As discussed and shown, the averaging method used in the present paper is not very accurate in the double discontinuous mode due to the inaccurate assumption of a piecewise linear signal shape. While our focus was extending the use of existing averaged models in transients that cross mode boundaries and not the development of a new averaging technique, these results suggest potential for improvement using more sophisticated averaging methods. Hence, in future work we plan to examine whether the Krylov-Bogoliubov-Mitropolski method already employed for CCM in Krein et al. (1990) results in more accurate mode-based averaged models.

REFERENCES

- Bacha, S., Munteanu, I., and Bratcu, A.I. (2014). *Power Electronic Converters Modeling and Control*. Springer, London.
- Ćuk, S. (1979). General topological properties of switching structures. In *1979 IEEE Power Electronics Specialists Conference*, 109–130. San Diego, CA, USA.
- Davoudi, A. and Jatskevich, J. (2007). Parasitics realization in state-space average-value modeling of PWM DC-DC converters using an equal area method. *IEEE Trans. Circuits Syst. I*, 54(9), 1960–1967.
- Erickson, R.W., Ćuk, S., and Middlebrook, R. (1982). Large-signal modelling and analysis of switching regulators. In *IEEE Power Electronics Specialists Conference*, 240–250.
- Heemels, W.P.M.H., Lehmann, D., Lunze, J., and De Schutter, B. (2009). Introduction to hybrid systems. In F. Lamnabhi-Lagarrigue and J. Lunze (eds.), *Handbook of Hybrid Systems Control: Theory, Tools, Applications*, 3–30. Cambridge University Press, Cambridge.
- Krein, P.T., Bentsman, J., Bass, R.M., and Lesieutre, B.L. (1990). On the use of averaging for the analysis of power electronic systems. *IEEE Trans. Power Electron.*, 5(2), 182–190.
- Lee, Y., Wang, S., and Hui, S. (1997). Modeling, analysis, and application of buck converters in discontinuous-input-voltage mode operation. *IEEE Trans. Power Electron.*, 12(2), 350–360.
- Li, A., Wang, Z., and Li, T. (2016). Mode transition approach for large signal average models of PWM DC-DC converters. In *6th International Conference on Electronics Information and Emergency Communication*, 232–235. Beijing, China.
- Maksimovi, D. and uk, S. (1991). A unified analysis of PWM converters in discontinuous modes. *IEEE Trans. Power Electron.*, 6(3), 476–490.
- Mao, Y.J., Lam, C.S., Sin, S.W., Wong, M.C., and Martins, R.P. (2018). Review and selection strategy for high-accuracy modeling of PWM converters in DCM. *Journal of Electrical and Computer Engineering*, 2018, 3901693.
- Middlebrook, R.D. and uk, S. (1977). A general unified approach to modelling switching-converter power stages. *International Journal of Electronics*, 42(6), 521–550.
- Sadarnac, D., Abida, W., and Karimi, C. (2004). The double discontinuous mode operation of a converter: a method for soft switching. *IEEE Trans. Power Electron.*, 19(2), 453–460.
- Sira-Ramírez, H.J. and Silva-Ortigoza, R. (2006). *Control design techniques in power electronics devices*. Springer, London.
- Sun, J. (2000). Unified averaged switch models for stability analysis of large distributed power systems. In *Fifteenth Annual IEEE Applied Power Electronics Conference and Exposition*, 249–255. New Orleans, LA, USA.
- Sun, J., Mitchell, D.M., Greuel, M.F., Krein, P.T., and Bass, R.M. (2001). Averaged modeling of PWM converters operating in discontinuous conduction mode. *IEEE Trans. Power Electron.*, 16(4), 482–492.